Vailable online at www.sciencedirect.com
SciVerse ScienceDirect
Energy Procedia 27 (2012) 319 – 324
Energy Procedia

SiliconPV: April 03-05, 2012, Leuven, Belgium

Silicon surface passivation by Al_2O_3: Recombination parameters and inversion layer solar cells

F. Werner[a]*, A. Cosceev[b], and J. Schmidt[a]

[a]Institute for Solar Energy Research Hamelin (ISFH), Am Ohrberg 1, 31860 Emmerthal, Germany
[b]Institute of Electronic Materials and Devices, Leibniz University Hanover, Schneiderberg 32, 30167 Hanover, Germany

Abstract

The interface between *p*- and *n*-type FZ-Si and an amorphous aluminum oxide (Al_2O_3) surface passivation layer deposited by plasma-assisted atomic layer deposition (ALD) was investigated by frequency-dependent conductance measurements. The hole capture cross section in the lower half of the bandgap, $\sigma_p = (4\pm3)\times10^{-16}$ cm^2, was found to be independent of energy. The electron capture cross section σ_n in the upper half of the bandgap decreases from $\sigma_n = (7\pm4)\times10^{-15}$ cm^2 at midgap over two orders of magnitude towards the conduction band edge. Numerical simulations of the effective surface recombination velocity based on these recombination parameters show a good agreement with experimental surface recombination velocities for a wide range of excess carrier and surface charge densities. Carrier transport in the inversion layer formed at the *n*-Si/Al_2O_3 interface was investigated yielding a sheet resistance of 15 kΩ/□, which was reduced to 6 kΩ/□ for a surface charge density of -2×10^{13} cm^{-2} obtained by corona charging. The applicability of Al_2O_3 inversion layers as emitters in *n*-type inversion layer solar cells was demonstrated by short circuit current densities of up to 25 mA/cm^2, which show a pronounced dependence on surface charge density.

Keywords: passivation; aluminum oxide; capture cross section; inversion layer solar cell;

1. Introduction

Aluminum oxide (Al_2O_3) deposited by atomic layer deposition (ALD) provides an outstanding level of surface passivation on both *n*- and *p*-type crystalline silicon [1,2] and is an ideal choice for the surface

* Corresponding author. Tel: +49-5151-999-314; fax: +49-5151-999-400.
E-mail address: werner@isfh.de.

doi:10.1016/j.egypro.2012.07.070

passivation of silicon solar cells [3,4]. A detailed knowledge of the energy-dependent electron-hole recombination parameters at the c-Si/Al_2O_3 interface enables highly predictive simulations of the interface recombination processes at the Al_2O_3-passivated solar cell surface, and hence would be of great benefit for the development and improvement of novel high-efficiency solar cells. In addition, an inversion layer forming at the surface of an *n*-Si wafer passivated with an Al_2O_3 film offers the opportunity to avoid a boron diffusion in the fabrication of *n*-type solar cells, as the inversion layer may act as charge collecting emitter in a novel *n*-type inversion layer solar cell as proposed in this contribution.

2. Interface recombination parameters

We measure the interface recombination parameters at the c-Si/Al_2O_3 interface as a function of the energetic position in the silicon bandgap using frequency-dependent conductance measurements [5] on metal-insulator-silicon (MIS) capacitors. The MIS-capacitors are fabricated on 1.3 – 1.5 Ωcm *p*-type and 1.5 Ωcm *n*-type FZ-Si wafers, respectively. The samples are coated on one side with 10 nm of Al_2O_3 deposited by plasma-assisted ALD. All samples are annealed for 15 min at 425 °C, then circular aluminum gate contacts are defined on top of the Al_2O_3 film by electron gun evaporation through a shadow mask, and a full-area aluminum back contact is evaporated on the non-coated side of the wafer. Figure 1(a) shows a sketch of the sample structure and the corresponding electric equivalent circuit. All relevant information about the interface recombination parameters is contained in the equivalent parallel conductance G_p, which is the conductive component of the interface-trap-related admittance Y_{it} in Fig. 1(a). The total admittance $Y_m(\omega)$ is measured as a function of the angular frequency ω at a fixed gate bias voltage V_G corresponding to a certain energetic position E_t in the silicon bandgap. Then G_p is extracted from $Y_m(\omega)$ and corrected for series resistance following a method described by Nicollian and Brews [6]. Figure 1(b) shows exemplary plots of the measured normalized parallel conductance G_p/ω as a function of ω for three different gate voltages V_G.

Figure 2 shows the capture time constants τ_p (below midgap, measured on *p*-type samples) and τ_n (above midgap, measured on *n*-type samples), the corresponding capture cross sections σ_p and σ_n, and the interface state density D_{it} deduced from the peak of G_p/ω as function of ω using the following relations:

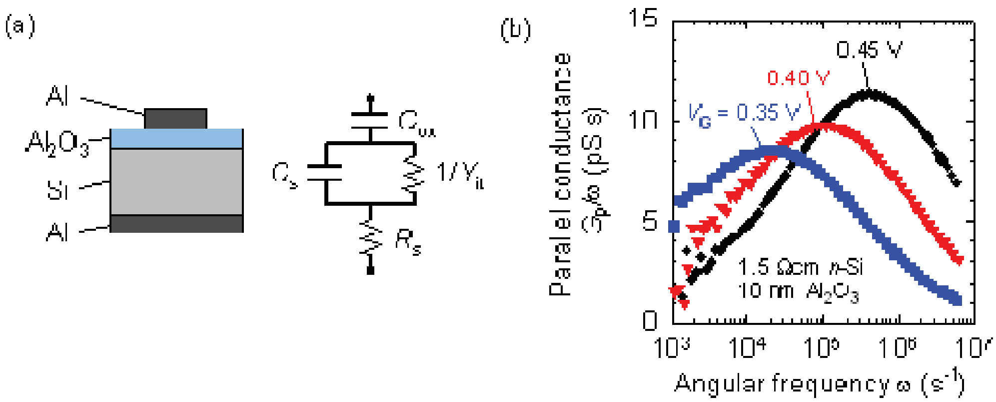

Fig. 1. (a) Sketch of the Al/Al_2O_3/Si capacitor (left) and corresponding electric equivalent circuit (right). (b) Exemplary plots of the normalized parallel conductance G_p/ω as a function of angular frequency ω for gate voltages of V_G = 0.35, 0.40, and 0.45 V on 1.5 Ωcm *n*-type FZ-Si for an Al_2O_3 film thickness of 10 nm.

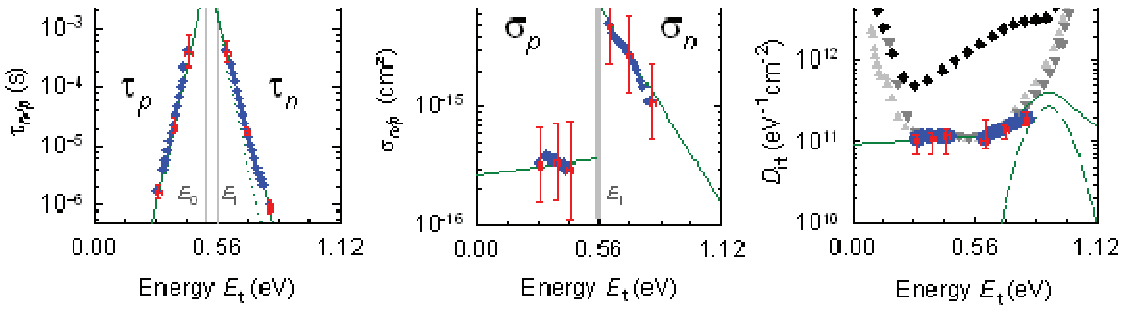

Fig. 2. (a) Capture time constants τ_p and τ_n as function of energetic position E_t in the silicon bandgap. The solid lines are exponential fits to the experimental data; the dotted lines illustrate the relation $\tau \propto \exp(\pm\beta E_t)$ expected for constant capture cross sections. (b) Capture cross sections σ_p and σ_n. The solid lines are calculated using the fit results from part (a). (c) Interface state density D_{it} obtained by the conductance method (circles) and by capacitance-voltage analysis on n-Si (triangles down), p-Si (triangles up), and on p-Si after applying a bias voltage of 3 V for > 5 min (black diamonds) leading to a degradation in D_{it}. The solid line shows the D_{it} distribution assumed for the numerical simulations in section 3. Error bars are shown in red for exemplary data points.

$$D_{it} \propto [G_p/\omega]_{peak}, \quad \tau_{n/p} \propto \omega_{peak}^{-1}, \quad \sigma_{n/p} \propto \tau_{n/p}^{-1} \exp(\mp \beta [E_t - E_i]), \tag{1}$$

where E_i is the intrinsic Fermi energy, $\beta = (k_B T)^{-1}$, k_B is the Boltzmann constant, and T is the temperature. A more detailed analysis of the data is presented in [7], a description of the method can be found in [6]. We obtain capture cross sections of $\sigma_n = (7\pm4)\times10^{-15}$ cm^2 and $\sigma_p = (4\pm3)\times10^{-16}$ cm^2 at midgap, which result in an asymmetry of $\sigma_n/\sigma_p = 5 - 70$. The hole capture cross section σ_p below midgap is virtually independent of energy, while the electron capture cross section σ_n above midgap decreases over two orders of magnitude towards to conduction band edge. It should be kept in mind, however, that small variations in the capture time constant lead to a large error in the capture cross section, which could conceal a more pronounced energy dependence of σ_p.

The interface state density D_{it} obtained by the conductance method is compared to D_{it} values obtained by capacitance-voltage (C-V) analysis [8]. Both methods are in excellent agreement and yield a virtually constant $D_{it} = (6–20)\times10^{10}$ $eV^{-1}cm^{-2}$ near midgap with a small Gaussian-shaped peak around an energy of 0.9 eV above the valence band edge [solid green line in Fig. 2(c)]. The steep increase in D_{it} towards the band edges shown in Fig. 2(c) is attributed to the impact of series resistance and inversion layer capacitance, which have been neglected in the analysis, and is hence neglected for numerical simulations.

3. Surface recombination velocity

We use an iterative numerical model presented by Girisch et al. [9], assuming flat quasi Fermi levels in the space charge region, and Shockley-Read-Hall (SRH) [10,11] theory to calculate the interface recombination velocity S_{it} at the c-Si/Al_2O_3 interface as a function of excess carrier density Δn, given by the following equation [9,10]:

$$S_{it} = \left(\frac{n_s p_s - n_i^2}{\Delta n} \right) \int_0^{E_g} \left[\frac{n_s + n_1(E_t)}{\sigma_p(E_t)} + \frac{p_s + p_1(E_t)}{\sigma_n(E_t)} \right]^{-1} v_{th} D_{it}(E_t)\, dE_t, \tag{2}$$

where $n_1(E)$ and $p_1(E)$ are the energy-dependent SRH-densities for a defect level at energy E_t [9], and n_s and p_s are the electron and hole concentrations at the interface. The resulting S_{it} is then folded with a Gaussian distribution of the surface charge density Q_Σ to account for spatial inhomogeneities of the field effect passivation. To verify the simulations we measure the effective carrier lifetime τ_{eff} as a function of excess carrier density Δn on *p*- and *n*-type FZ-Si samples passivated on both sides with Al_2O_3 layers deposited by plasma-assisted ALD. The effective surface recombination velocity (SRV) S_{eff} is then calculated from τ_{eff} using the equation [12]:

$$S_{\mathrm{eff}} = \frac{w}{2}\left[\left(\tau_{\mathrm{eff}} - \frac{w^2}{\pi^2 D}\right)^{-1} - \tau_{\mathrm{b}}^{-1}\right], \quad (3)$$

where *w* is the wafer thickness, *D* is the minority carrier diffusion constant, and τ_b is the bulk lifetime. For τ_b we use an empirical parameterization [13], which accounts for intrinsic radiative and Auger recombination. Further losses, e.g. recombination via bulk defects, are neglected. Hence we obtain an upper limit $S_{eff.max}$ of the surface recombination velocity.

The conductance method is only sensitive to majority carriers, and hence the capture cross sections σ_p and σ_n are only known in one half of the bandgap. We replace the unknown values of $\sigma_{n/p}$ by the midgap values of σ_n and σ_p, as the choice of model only has a small effect on the calculated S_{it} [7].

Due to the excellent field-effect passivation caused by the high negative fixed charge density $Q_f = -(4\pm1)\times10^{12}$ cm^{-2} at the c-Si/Al_2O_3 interface [8], interface recombination is strongly suppressed. We gradually compensate Q_f by corona charging, the total surface charge density Q_Σ is then given by the sum of Q_f and the deposited corona charge density Q_c. Figures 3(a) and (b) show the numerically calculated (lines) and experimentally determined (symbols) injection-level-dependent effective SRV $S_{eff}(\Delta n)$ for 1.3 Ωcm *p*-Si and 1.0 Ωcm *n*-Si, respectively, for different exemplary Q_Σ values. The calculated S_{eff} values include the interface recombination velocity S_{it} and, in order to explain the injection level dependence of the lower plot ($Q_\Sigma = -3.8\times10^{12}$ cm^{-2}, black line), an increased recombination in the space

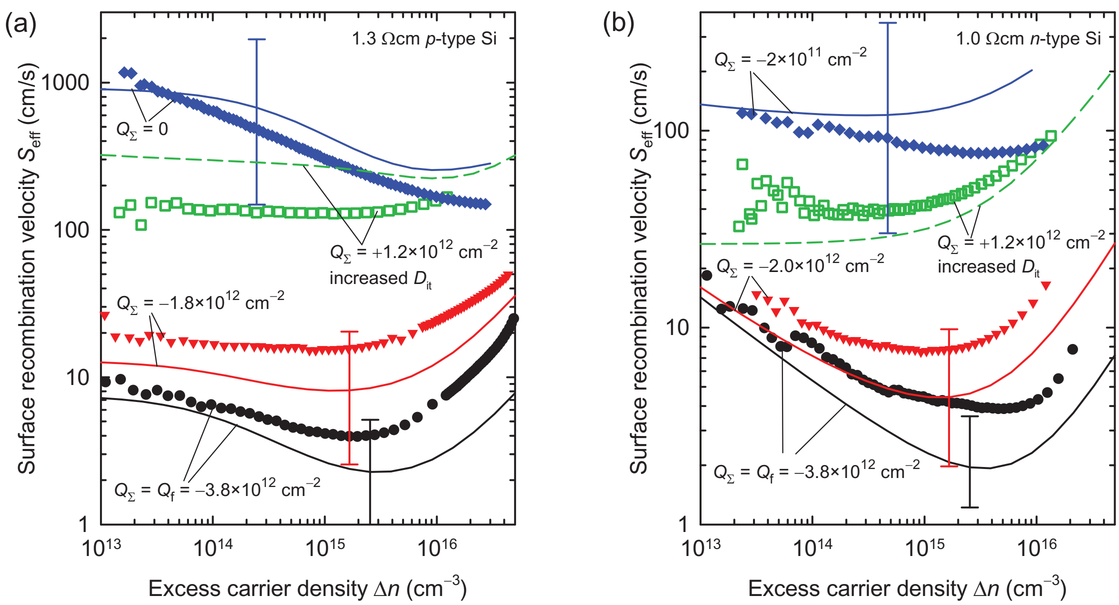

Fig. 3. Calculated (lines) and experimentally determined (symbols) effective SRV S_{eff} for (a) 1.3 Ωcm *p*-Si and (b) 1.0 Ωcm *n*-Si as a function of excess carrier density Δn for different negative (closed symbols) and positive (open symbols) surface charge densities Q_Σ given in the plot. The green dashed lines are calculated assuming an increased interface state density D_{it}, in order to account for interface damage induced during excessive corona charging. No error bar is given due to this assumption.

charge region [14,15]. At low $|Q_\Sigma|$ values interface recombination dominates and recombination in the space charge region becomes negligible. The calculated $S_{eff}(\Delta n)$ curves are in excellent agreement with the experimental data, taking into account that recombination via bulk defects has been neglected. However, we observe two exceptions: (i) For Q_Σ near zero, S_{eff} seems to be systematically overestimated, although calculation and experiment agree within the uncertainty. For Q_Σ near zero S_{eff} is sensitive to small changes in Q_Σ of the order of 10^{11} cm^{-2}, which is below the smallest charging step of $\Delta Q_c \approx 5\times10^{11}$ cm^{-2} in our experimental setup. Hence, a slight deviation from $Q_\Sigma = 0$ or assuming a larger inhomogeneity of the deposited corona charge is expected to lead to a better agreement. (ii) As previously shown in Ref. 7, S_{eff} is significantly underestimated for large values of $Q_\Sigma > +10^{12}$ cm^{-2}. We attribute this to damage occurring during corona charging, as the same effect is observed for both *p*- and *n*-type samples, and hence is unlikely to be related to the charge polarity. This interpretation is supported by our experimental finding that after removal of the corona charges using deionized water the carrier lifetime is reduced compared to the initial lifetime of the sample. Assuming an increased interface state density D_{it}, which we measured after degrading the c-Si/Al_2O_3 interface by applying a large bias voltage [black diamonds in Fig. 2(c)], leads to a good agreement between calculated and experimental S_{it} values for $Q_\Sigma = +1.2\times10^{12}$ cm^{-2}.

4. Inversion layer solar cell

Due to the negative fixed charge density at the c-Si/Al_2O_3 interface, an inversion layer forms at the surface of an *n*-Si wafer passivated with an Al_2O_3 film, which may be applied as emitter in *n*-type inversion layer solar cells. Figure 4(a) shows the sheet resistance $R_\square$ of the inversion layer determined by the transition line method (TLM) as a function of surface charge density Q_Σ, with values ranging from $R_\square$ = 15 kΩ/□ for $Q_\Sigma = Q_f = -3.8\times10^{12}$ cm^{-2} down to 6 kΩ/□ for $Q_\Sigma = -2\times10^{13}$ cm^{-2}. For a contact spacing of 200 µm, these $R_\square$ values correspond to a series resistance contribution of 0.2 – 0.5 Ωcm^2, sufficiently low to make an inversion emitter formed by Al_2O_3 deposition feasible. Figure 4(b) shows a sketch of a 165 µm thick 2×2 cm^2 inversion layer solar cell fabricated on 1 Ωcm *n*-type Cz-Si with a non-optimized front finger spacing of 280 µm. The short circuit current density J_{sc} measured under standard test conditions (AM1.5G, 100 mW/cm^2, 25 °C) is shown as blue squares in Fig. 4(a) as a function of Q_Σ, yielding values of up to 25 mA/cm^2. The pronounced dependence of J_{sc} on Q_Σ is strong evidence that the inversion layer is indeed acting as charge collecting emitter in the solar cell. Further experiments at our lab will reveal the full potential of Al_2O_3-induced inversion layers for *n*-type Si solar cells.

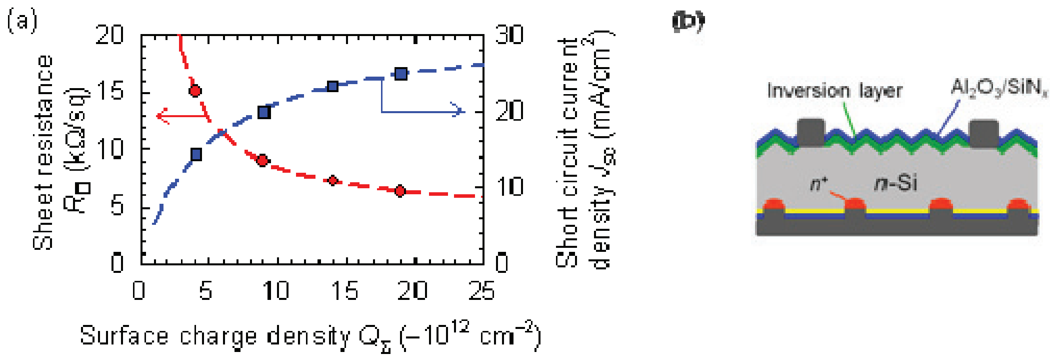

Fig. 4. (a) Inversion layer sheet resistance $R_\square$ determined by TLM (red circles) and short circuit current density J_{sc} measured under standard test conditions (AM1.5G, 100 mW/cm^2, 25 °C) on 2×2 cm^2 Al_2O_3 inversion layer solar cells (blue squares) as a function of surface charge density Q_Σ. The lines are guides to the eye. (b) Sketch of the Al_2O_3 inversion layer solar cell fabricated on *n*-Si.

5. Conclusions

The interface between *p*- and *n*-type FZ-Si and an amorphous Al_2O_3 surface passivation layer deposited by plasma-assisted ALD was investigated by conductance measurements. The hole capture cross section in the lower half of the bandgap, $\sigma_p = (4\pm3)\times10^{-16}$ cm^2, was found to be independent of energy. The electron capture cross section in the upper half of the bandgap on the other hand decreases from $\sigma_n = (7\pm4)\times10^{-15}$ cm^2 at midgap over two orders of magnitude towards the conduction band edge E_c. The capture cross section ratio at midgap is highly asymmetric with $\sigma_n/\sigma_p = 5 – 70$. The interface state density D_{it} shows an excellent agreement with values obtained from capacitance-voltage analysis, yielding D_{it} values around the middle of the bandgap of the order of 10^{11} eV^{-1}cm^{-2}. Numerical calculations of the injection level dependent surface recombination velocity based on these interface recombination parameters for Al_2O_3-passivated samples show a good agreement to experimental data for both *n*- and *p*-Si and for a wide range of surface charge densities. However, the interface quality is shown to degrade after deposition of large corona charge densities. We determine a sheet resistance of $R_\square = 15$ kΩ/□ for the inversion layer formed at the *n*-Si/Al_2O_3 interface, which was reduced to 6 kΩ/□ by corona charging. We propose a novel *n*-type inversion layer solar cell, where the emitter consists of an inversion layer formed by depositing an Al_2O_3 layer on top of the *n*-type Si. We obtain short circuit current densities up to 25 mA/cm^2, which show a strong dependence on surface charge density, clearly demonstrating the feasibility of an *n*-type inversion layer solar cell formed by Al_2O_3 deposition.

Acknowledgements

Funding was provided by the State of Lower Saxony and the German Ministry for the Environment, Nature Conservation and Nuclear Safety (BMU) under contract number 0325050 (“ALD”).

References

[1] Agostinelli G, Delabie A, Vitanov P, Alexieva Z, Dekkers H, Wolf SD, Beaucarne G. *Solar Energy Materials & Solar Cells* 2006;**90**;3438.

[2] Hoex B, Heil S, Langereis E, van de Sanden MCM, Kessels WMM. *Applied Physics Letters* 2006;**89**;042112.

[3] Schmidt J, Merkle A, Brendel R, Hoex B, van de Sanden MCM, Kessels WMM. *Progress in Photovoltaics: Research and Applications* 2008;**16**;461.

[4] Benick J, Hoex B, van de Sanden MCM, Kessels WMM, Schultz O, Glunz SW. *Applied Physics Letters* 2008;**92**;253504.

[5] Nicollian EH, Goetzberger A. *Bell Systems Technical Journal* 1967;**46**;1055.

[6] Nicollian EH, Brews JR. *MOS Physics and Technology*. New York: Wiley;1982; pp. 208–225.

[7] Werner F, Cosceev A, Schmidt J. *Jornal of Applied Physics* 2012;**111**;073710.

[8] Werner F, Veith B, Zielke D, Kühnemund L, Tegenkamp C, Seibt M, et al. *Journal of Applied Physics* 2011;**109**;113701.

[9] Girisch R, Mertens R, de Keersmaecker R. *IEEE Transactions on Electron Devices* 1988;**35**;203.

[10] Shockley W, Read WT. *Physical Review* 1952;**87**;835.

[11] Hall RN. *Physical Review* 1952;**87**;387.

[12] Sproul AB. *Journal of Applied Physics* 1994;**76**;2851.

[13] Richter A, Werner F, Schmidt J, Glunz SW, Cuevas A. *Energy Procedia* 2012;in press.

[14] Dauwe S, Schmidt J, Metz A, Hezel R. *Proc. 29th IEEE PVSC*, New Orleans, LA (IEEE, New York, 2002), p. 162.

[15] Steingrube S, Altermatt PP, Zielke D, Werner F, Schmidt J, Brendel R. *Proc. 25th EUPVSEC*, Valencia, Spain (WIP, Munich, Germany, 2010), p. 1748.